Composition Design of Nanocrystalline Bainitic Steels by Diffusionless Solid Reaction

Carlos Garcia-Mateo[1], Francisca G. Caballero[1], Thomas Sourmail[2], Juan Cornide[1,3], Veronique Smanio[2], Roberto Elvira[4]

[1] National Center for Metallurgical Research (CENIM-CSIC), Department of Physical Metallurgy. MATERALIA Research Group. Avda. Gregorio del Amo, 8, 28040, Madrid, Spain.

[2]Ascometal-CREAS (Research Centre) Metallurgy, BP 70045 57301 Hagondange Cedex, France.

[3] Université de Rouen, GPM UMR6634, BP12, 76801 St-Etienne-du-Rouvray, France

[4]Gerdau I+D EUROPA S. A. Barrio Ugarte, 48970 Basauri, Spain

Corresponding Author: Carlos Garcia-Mateo. cgm@cenim.csic.es.

ABSTRACT

NANOBAIN is the term used to refer to a new generation of advanced steels capable of producing by isothermal transformation at low homologous temperatures, $T/T_m \sim 0.25$ where T_m is the absolute melting temperature, a nanocrystalline microstructure, composed exclusively of two phases, thin plates of bainitic ferrite separated by C enriched austenite. Such alloys are exclusively designed on the basis of bainitic transformation theory and some physical metallurgy principles. In this work, by designing a new set of alloys capable of producing such microstructure, a further step toward the industrialization of NANOBAIN is taken. Some important industrial requirements, including circumventing the inclusion of expensive alloying elements and the need for faster transformations, are also considered. For all the alloys, the experimental results validate the design procedure and they illustrate that the NANOBAIN concept is a step closer to industrialization, probing that it is possible to obtain nanocristalline bainite in simpler alloy systems and in shorter times than those reported previously.

Keywords: nanostructured materials, tempering, phase transformation, dilatometry, bainite

1.INTRODUCTION

The term bainite refers to the product of decomposition of austenite (γ) at temperatures between those at which pearlite and martensite form. The diffusionless, displacive mechanism theory describing bainitic transformation states that bainitic transformation occurs via paraequilibrium nucleation, where only C diffuses, and by displacive difussionless growth. Furthermore, there is no change in the chemical composition between the parent and product phase. Thermodynamically these conditions are expressed as $\Delta G_m < G_N$ and $\Delta G^{\gamma\to\alpha} < -G_{SB}$, respectively. Here, ΔG_m is the maximum free energy change accompanying the nucleation under paraequilibrium conditions and G_N is the universal nucleation function based on a dislocation mechanism associated with martensite [1-4], and it defines the minimum free energy change necessary in any steel, in order to nucleate bainite. $G_{SB} \cong 400$ J/mol is the stored energy of bainite; $\Delta G^{\gamma\to\alpha}$ is the free energy change of the transformation of γ without any change in chemical composition [3]. The temperature at which both conditions, nucleation and growth, are fulfilled is known as the bainite start temperature, B_S. Soon after the diffusionless growth of a bainitic ferrite subunit is completed, the excess C is partitioned to the surrounding austenite. This process continues by successive nucleation of subunits until the C concentration of the residual austenite reaches the value at which the free energy of bainite is less than that of austenite of the same composition. The transformation then stops because it is thermodynamically impossible for austenite of such chemical composition to transform to bainite by the aforementioned mechanism. This trend is known as the 'incomplete reaction phenomenon' because the transformation ends before the C concentration of austenite reaches the equilibrium value. These phenomena can be encompassed by the concept of the T_o' curve, which is the locus of points on a temperature versus C concentration plot where austenite and ferrite of the same

chemical composition have the same free energy, taking into account the stored energy of the ferrite due to the displacive mechanism of transformation (400 J/mol) [4,5].

It is possible to design steels that transform to a nanostructured carbide free bainite, also known as NANOBAIN, relying solely on this phase transformation theory and well known metallurgical features. This type of microstructure was achieved in early studies by chemical composition control, seeking homologous temperatures as low as $T/T_m \approx 0.25$, where T_m is the absolute melting temperature [6,7]. But the transformation required more than 2 months to be completed at 125 ºC, and about 10 days at 200 ºC. Further research allowed a substantial decrease of the transformation time, 3 days at 200 ºC, and even finer bainitic microstructures [8]. This improvement relies in two concepts: control of the austenitisation conditions previous to bainitic transformation and the addition of Co and/or Al. Both of these elements are known for increasing the free energy change for transformation [9], or in other words, for accelerating transformation kinetics.

Steelmakers and final users appreciated the mechanical properties [10,11] and the impressive improvement in transformation kinetics, but joint efforts between the scientific, industrial, and final user community have only reported a limited set of relevant parameters to consider during the design process, i.e. a blueprint for a new generation of NANOBAIN alloys. These parameters can be summarized as follows:

- A simple alloy system: to avoid being limited to niche applications, the alloys must be cheap to produce; i.e. raw materials such as Co and Ni are ruled out from the design as is high Al addition due to the cleanliness requirements of ultra-high strength steels and researchers instead are seeking an inexpensive and lean system such as Fe-C-Si-Mn-Cr.

- Carbide free microstructure. The presence of coarse cementite, a hard and brittle phase, may impair future mechanical properties. It is therefore imperative to retard and to some extent avoid its precipitation from austenite during bainite reaction. For this purpose, Si was originally added to the chemical composition in quantities of at least 1.5 wt.% [12].

- Reducing the transformation temperature range at which austenite transforms into bainite, $M_S < T < B_S$, is a way to attain higher fractions of finer bainitic ferrite plates [13]. It can also enhance the thin film morphology of retained austenite as opposed to blocky [14].The benefits of this can be found in strength and toughness.

- The rate of reaction is also an important industrial requirement, since the transformation must be achieved in a realistic time. A relevant approach can be a thermodynamic (chemical composition control) technique and/or reduction of the prior austenite grain size, PAGS, as in ref. [8].

- Hardenabillity. The heat treatment consists of austenitization at a given temperature, above A_{C3}, followed by quenching to a temperature above Ms, where the component is held for a duration sufficient to achieve the maximum volume fraction of bainite. A conventional quenching process is thus not applicable, and dry bainitizing (DryBainTM) [15] for small components of 200x20x30 mm^3 and a salt bath for larger specimens of 700x400x250 mm^3 are used instead. For all sizes, and especially larger components, the transformation should take place in a controlled manner throughout the component. It is therefore essential that, even at the slowest cooling point of the component, the cooling rate be sufficient to avoid formation of ferrite/pearlite or other transformation products during continuous cooling. Based on a combination of experimental studies and in-house simulation tools, the cooling rate of the biggest component during salt bath bainitizing was estimated as approximately 1.5°C/s. It was thus concluded that the adapted steel grade should be designed so as not to form ferrite/pearlite for cooling rates faster than 1.5 ºC/s.

-Additional refinement of the microstructure. The aim of is to retain the nano-scale by acting directly on the strength of the parent austenite where bainitic ferrite grows, instead of increasing the free energy change for transformation, as in the case of the Co and Co+Al alloys in ref. 8. It is thus thought that Si addition should be increased up to 2.9 wt.% and Mo to 0.1wt.% to obtain further strengthening of the austenite prior to the bainite reaction. According to Ref. 16, an increase of 1 wt.% of Si implies an

increase of 4% of the YS of austenite, while a 0.1 wt.% increase of Mo represents a 0.3% increase of the YS.

Bearing these industrial demands in mind and using Co and Co+Al alloys as benchmarks, in terms of properties, microstructure, and transformation times, a new set of low temperature bainitic steels have been designed. The design procedure is based solely on a combination of thermodynamic and kinetics models together with some physically metallurgy principles [17-20] with the final aim of taking the first step towards its industrialization. The experimental work presented in this study also validates the theoretical alloy design process.

2. EXPERIMENTAL PROCEDURE

The chemical compositions of the designed alloys are listed in Table 1. All the alloys belong to the system Fe-C-Si-Mn-Cr except for small Mo and Nb additions. As stated, low B_S and M_S temperatures can be achieved using high carbon concentration and, to a lesser extent, solutes such as Mn and Cr, which in the present context increase the stability of austenite relative to ferrite. But, as high C content slows down the transformation kinetics, it was also assumed in some of the alloys that a decrease of the C content down to 0.8 or 0.6 wt.%. In the 0.6 alloys in particular the decrease in the C content was compensated, in terms of B_S and M_S, with higher Mn and Cr contents compared with the other alloys. As one of the premises of the design process is to use viable alloying elements, Co (due to its price) and Al (because it incompatible with cleanliness requirements of ultra-high strength steels), both originally present in the benchmark alloys (B.A.) [8], were excluded from the new system. Their accelerating capability on bainitic transformation was compensated by keeping Cr and Mn as low as possible so as to maintain the transformation times within the range of the Co and Co+Al alloys [8], and, at the same time, to ensure

sufficient hardenability to avoid transformation during cooling from the austenitization temperature to the bainite transformation temperature.

All the alloys without exception contain sufficient silicon (at least 1.5 wt.%) to suppress precipitation of cementite from austenite. Nb addition of 0.03 wt.% is carried out to refine the austenite grain size and thus further accelerate the bainitic transformation of alloys 1CNb and 0.6CNb. In order to promote even smaller bainite plate thickness, an increase in the strength of austenite, from where bainitic ferrite will grow, additions of 0.1 wt.% of Mo or 2.5 wt.% extra Si were carried out for some of the alloys, i.e. 1CMo, 0.6CMo, and 1CSi.

The laboratory grade specimens were induction melted under vacuum, and then cast into rectangular ingots of approximately 20-35 kg. The lower and upper parts of the ingots were then discarded and the remainder was hot forged into bars of 40-50 mm in a temperature range of 1200-1250 ºC. For the 1CSi cast, the forging temperature was kept as low as possible (1025 ºC) in order to avoid burning. In all cases, in order to avoid the possibility of cracking during natural cooling, the laboratory casts were slow cooled after forging and then annealed in a furnace at 700-650 ºC to allow handling and machining.

An Adamel Lhomargy DT1000 high-resolution dilatometer was used to construct the CCT diagrams, obtain the critical transformation temperatures upon heating, and to perform all the isothermal heat treatments. The dimensional variations of the specimen are transmitted via an amorphous silica pushrod and measured by a linear variable differential transformer (LVDT) in a gas-tight enclosure, enabling tests under vacuum or in an inert atmosphere. The DT1000 dilatometer is equipped with a radiation furnace for heating. The energy radiated by two tungsten filament lamps is focused on a cylindrical specimen of 2mm diameter and 12mm length by means of a bi-elliptical reflector. The temperature is measured with a 0.1mm diameter chromel-alumel (type K) thermocouple spot welded to the specimen. The high efficiency

of heat transmission and the very low thermal inertia of the system ensure that constant heating rates ranging from 0.003 to 200 ºCs^{-1} can be achieved.

To reveal the microstructure, metallographic samples were cut, ground, and polished following the standard procedures. A 2% Nital etching solution was used to reveal the bainitic microstructure, and observations were carried out on a JEOL J8M-6500 field emission gun scanning electron microscope (SEM-FEG) operated at 10 kV. Before etching, the samples were polished using a colloidal silica suspension. High magnification SEM-FEG micrographs were used to determine the distribution and size of the different retained austenite morphologies as well as the bainitic ferrite plate thickness *t*, by measuring the mean lineal intercept $\overline{L}_T = \pi t / 2$ in a direction normal to the plate length [8, 21]. Prior austenite grain size (PAGS) was revealed using a thermal etching technique described in reference [22,23].

A quantitative X-ray diffraction analysis was carried out to determine the fractions of retained austenite (V_γ) and bainitic ferrite (V_α). For this purpose, samples were machined, ground, and finally polished using a colloidal silica suspension. They were then step-scanned in a SIEMENS D5000 X-ray diffractometer using unfiltered Co K_α radiation. The scanning speed (2θ) was less than 0.3º/min. The machine was operated at 40 kV and 30 mA. The volume fraction of retained austenite was calculated from the integrated intensities of (200), (220), and (311) austenite peaks, and those of (002), (112), and (022) planes of ferrite [24].

TEM specimens were sliced from 3-mm-diameter rods of the heat-treated material, mechanically thinned to 0.06 mm, and then twin-jet electropolished to perforation using a mixture of 5% perchloric acid, 25% glycerol, and 70% ethanol at 10 ºC and 45 V. The samples were examined on a TEM JEOL 2010 transmission electron microscope operated at 200 keV.

Theoretical calculations regarding phase diagrams and also the evolution of Nb carbides with temperature were performed with the help of a commercial package for thermodynamic calculations in equilibrium in combination with the SGSOL-SGTE Solution database [25].

Hardness was measured as HV and the presented results correspond to an average of at least 3 values.

3.KINETICS OF BAINITE TRANSFORMATION

The bainitizing heat-treatments consist of austenitizing at temperatures above A_{C3} (or A_{Cm} for hypereutectoid steels) followed by "rapid" cooling to the required isothermal transformation temperature, $M_S < T < B_S$, where M_S and B_S represent the martensite and bainite start temperature. The rate of cooling should depend on the hardenability of the steel grade, because the only requirement is to avoid transformation during cooling.

Therefore, the important temperatures that should be determined for the design of the heat treatment are: (i) A_{C1}, A_{C3}/A_{Cm} to determine suitable austenitising conditions; (ii) M_S to ensure that bainitizing can be carried out above this temperature; and (iii) the critical cooling rate below which transformation occurs during continuous cooling, for which CCT diagrams are needed. In the second step, TTT diagrams in the bainitic temperature range are constructed to determine the duration of bainite transformation as a function of the temperature. This was also carried out using high resolution dilatometry.

According to thermodynamic calculations, the 1C & 0.8C alloys are hypereutectoid (see for example the isopleth diagram in Fig. 1). This implies that, unless avoided during the casting process, the presence of primary cementite may jeopardize the final mechanical properties of the bainitic microstructure. This phase, once precipitated at high temperatures, is very stable and is extremely difficult to dissolve. Another argument to avoid at all instances its presence is, that for the theoretical calculations performed during the design process of these alloys, it was assumed that the bulk material chemical composition and the composition of the austenite before the onset of the bainitic microstructure were identical. As a C rich

phase, the presence of primary cementite substantially changes the chemical composition of the austenite, meaning that the calculations, i.e. the whole design process, become inaccurate.

It is impossible to manipulate the solidification parameters of experimental ingot casting to avoid primary carbide precipitation, as solidification of the ingot has natural cooling without extra cooling. The only option is to reduce the casting temperature, but this is quite difficult in a laboratory setting. Therefore, the material for this study was taken at mid-radius, avoiding the central part of the bars and originally from the ingot, and therefore the presence of primary cementite was not observed in any of the alloys after casting.

Experimental determination of the Ac1 and Ac3 temperatures, listed in Table 2, was performed on dilatometry curves obtained during heating to 1100 ºC for all grades. According to the listed results, the austenitization temperature (T_γ) for the 1C and 0.8C alloys was selected as 950ºC, while for the 0.6C alloys it was set at 890 ºC, and the time for austenitisation was fixed at 15 min for all cases. Temperatures that were as low as possible to avoid exaggerated austenite grain growth, which would retard bainitic transformation kinetics, but high enough to ensure complete austenitization were selected.

3.1CCT diagrams

CCT diagrams determined for the selected T_γ temperatures are presented in Fig.2 Different cooling temperatures from T_γ to room temperature were selected, i.e. 1.5-3-5-10-20-50 ºC/s. The reported Ac1 and Ac3 were experimentally obtained from the heating dilatometric curves. As shown in Table 2, and as expected, the M_S temperatures for the high C alloys (1C & 0.8C) are significantly below those for the 0.6C grades. The isothermal temperatures will therefore be limited to 250 ºC for the 0.6C grades.

In terms of hardenability, the critical cooling rate (CR) of the 1-0.8C alloys is largely below that of the 0.6C alloys, which is close to 3-5ºC/s. Also, as expected, bainite is not obtained by continuous cooling in

any of the alloys. It is interesting that pearlite transformation is enhanced with increasing C content, a result that contradicts equilibrium theoretical calculations. However, this is in line with the finding that as the alloy becomes hypereutectoid the austenite becomes less stable with respect to cementite precipitation and transformation to pearlite becomes faster [26,27]

3.2. Isothermal heat treatments and basic microstructural characterization

For the isothermal heat treatments the cooling rate from T_γ was adapted to the steel grade investigated to ensure that no other transformation interferes with bainitic transformation. It was therefore on the order of 10 ºC/s for the 0.6C alloys and 30 ºC/s for the 1-0.8C grades; see Table 2. Figure 3 shows the typical appearance of the dialtometric signal during isothermal transformation at different temperatures. It is worth noting that as the temperature increases, shorter time is needed to reach a superior plateau, i.e. end of bainitic transformation. In addition, the strength of the signal ($\Delta L/Lo$) is weaker, implying that less bainitic ferrite is formed.

Determination of the time needed to end bainitic transformation was made on curves of the type shown in Fig. 3. The criterion to estimate the end of transformation is schematically represented in Fig. 4. The end of the transformation was fixed at the point where the first derivate (transformation rate) achieved null variation. Figure 4 shows two cases, one where the null point criteria is (0.6CMo 260 ºC) and another where it is not accomplished (0.6CNb 220 ºC) (Fig. 4 (a) and (b), respectively). While this procedure might seem irrelevant, it is necessary to highlight that after a fast increase in the dilatometric signal, the approach of a steady state or plateau (i.e., no further transformation) might not be evident. Two main different scenarios have been observed: i) one where the signal steadily and slowly increases and never reaches horizontality; and ii) another where even after reaching a plateau it decreases slightly (see the

curves in Fig. 3). Far from being related with the transformation per se, these abnormalities of the dilatometric signal are a consequence of, and consistent with, small changes in the temperature during long heat treatment, of both, dilatometer´s components in contact with the sample and also the walls of the vacuum chamber. In the case of the 0.6CMo, two different times were marked, 25530s as the time when the derivate becomes null and 31875s as the time when the plateau is reached. Calculations indicate that the increase of the bainitic ferrite fraction from one time to the other will be on the order of the uncertainty of X-ray experiments, used to determine the bainite fraction, ± 3%, but the time difference between one process and the other is 1.7h.

Based on that approach, transformation durations at the different temperatures investigated are shown in Fig. 5 and Fig. 6 together with the corresponding hardness. According to the data in Table 2 for the 1C & 0.8C grades, the isothermal heat treatments were limited to a range of 200-350 ºC while for the 0.6C alloys they were limited to 250-350 ºC, when doable. Regardless of the alloy chemical composition, in all the presented isothermal experiments the microstructure consisted of a mixture of two phases, bainitic ferrite (α) and carbon enriched regions of austenite (γ). Figure 7 show optical micrographs of the microstructure obtained after isothermal heat treatments at 220 and 300 ºC of the 1C alloy. The new nanostructures require a re-definition of the term block. In this sense, the lighter phases in Fig. 7 are micro-blocks of retained austenite (> 1000 nm), whereas the darker feather-like features are sheaves of bainite, groups of bainitic ferrite plates sharing a common crystallographic orientation and separated by thin films of retained austenite. It is clear that as the transformation temperature increases the amount of retained austenite increases, as does the proportion of micro-blocks as compared with the thin films [9]. Therefore, the general terminology used in conjunction with the development of new low temperature bainitic steels, describing blocks of austenite as pools of this phase trapped between sheaves of bainite, several tens of microns large and easily observable under light optical microscopy, is no longer applicable. At much higher magnification, as seen Fig. 8, it is possible to observe the bainitic ferrite plates

(lower relief) and the retained austenite (higher relief) as sub-micron blocks (100-1000 nm) and nano-films (< 100nm).

Plastic relaxation of the shape change occurring as a consequence of the displacive growth of bainite takes places via generation of dislocations in the austenite/bainitic ferrite interface, as shown in Fig. 9, where extensive dislocation debris is evident in a sub-micron block of retained austenite, and also via micro/nano twins in the austenite in contact with bainitic ferrite plates [28-32].

As expected from the high C content of all the grades and the additional C enrichment at which austenite is subjected during bainitic transformation, martensitic transformation has not been detected in dilatometry during cooling to room temperature. This supports that in all cases the microstructure consisted exclusively of bainitic ferrite and C enriched retained austenite.

In terms of the 1C & 0.8C bainite transformation kinetics, as presented in Fig. 5, the transformation moves from very sluggish at the lowest temperature, 200 ºC, 55-40 h, to very fast at 350 ºC, where transformation only requires 3-6 h. This same trend is observed for the 0.6C family. In general terms the alloys exhibit faster transformation kinetics than their higher C counterpart. The difference becomes greater as the transformation T increases; e.g. at 350 ºC no more than 2h is needed to finish the transformation, while at 300 ºC the time needed is similar to that of the 1C & 0.8C.

The detailed variation of hardness as a function of the transformation temperature is illustrated in Fig. 5 and Fig. 6. Each hardness point on the graph represents a mean of at least three measurements, with a typical variation of only ±10 HV. The progressive hardness decrease as transformation temperature increase responds to the expected increase of retained austenite at the expense of bainitic ferrite and the thickening of ferrite plates [6], as it will be proved shortly. It is remarkable that the HV of the fully transformed microstructures at the lowest transformation temperatures compares well with those of the quenched microstructures, 50 ºC/s in Fig. 2, which is a mixture of retained austenite and martensite. For

the quenched microstructures and average values of 820 HV and 770 HV for the 1C & 0.8C and 0.6C families can be considered. Comparing the newly designed alloy´s results with those of the benchmark alloys (B.A.), denoted by the dotted lines in Fig. 5 and Fig. 6, the achievement of harder microstructures, even for the 0.6C case, is evident.

Table 3 summarizes the results from the detailed characterization of selected microstructures. As expected, in all cases, bainitic ferrite is the main phase, and its presence represents almost 75% of the total content for all the alloys except for the 1CSi, where it is 65%, the remaining being retained austenite V_{γ}. Table 3 confirms that bainitic ferrite plate is within the nano-range, and it is possible to distinguish between two sets of data. The 0.6C family have plate thickness ranging from 43-65 nm, being the thinnest among those corresponding to stronger austenite, i.e. alloys with Mo and Cr. The other set of alloys, 1C & 0.8C, have a plate thickness that is almost half of that reported for the 0.6C alloys, i.e. ranging from 21-39 nm. It is interesting that a decrease in the transformation temperature does not lead to further refinement in the microstructure, according to reports thus far.

Considering that the retained austenite thin films are intimatley mixed with bainitic ferrite plates, refinement of the microstructure down to the nanoscale is also attained in the austenite, as shown in Fig. 8 and Fig. 9. As an example, two populations of the 1CSi alloys were studied at 220 and 250 ºC, and the results are presented in Fig. 10. The nano-films have an average thickness of ~35 nm for both heat treatments and exhibit very similar size distributions. However, an increase in the isothermal temperature leads to both coarser blocks of austenite, from 630 to 870 nm at 220 and 250 ºC, respectively, and a wider distribution towards larger sizes.

4.VALIDATION OF BLUEPRINT DEFINITION

The blueprint for the design of the new generation of NANOBAIN alloys is the result of scientific and industrial joint efforts to identify the most relevant parameters to be considered. In this section we evaluate the level of fulfilment of those parameters as a means of validating the design process.

4.1Simple system Fe-C-Si-Mn-Cr

For viability and economic reasons the authors explored the possibility of obtaining NANOBAIN microstructures in very simple and inexpensive systems, avoiding the inclusion of expensive raw materials as Co and Ni. High Al addition was also avoided in order to meet cleanliness requirements.

Table 1 summarizes the designed alloys belonging to the system Fe-C-Si-Mn-Cr, where small additions of Mo and Nb were justified for other means.

4.2Carbide-free microstructure

When advanced bainitic steels are designed, the presence of cementite, a hard and brittle phase that impairs the mechanical properties, should be avoided. Addition of judicious quantities of Si to the chemical composition, at least 1.5 wt%, impedes the precipitation of cementite from austenite. After extensive high magnification SEM and TEM observations of the microstructures, it was confirmed that indeed cementite was not present.

4.3Low transformation temperatures

Lowering the transformation temperatures provides several benefits, as presented in this work. Based on previous experience and results it was decided that transformations temperatures for the new alloys should be as close as possible to those of the benchmark alloys [8] i.e. between 200-350 ºC. For the newly designed alloys and the reference alloys in the NANOBAIN family [6,8], Fig. 11 summarizes the

experimental M_S and the maximum tested temperature where bainite was obtained. The exact value of B_S has not been obtained. From the results the goal of keeping transformation temperatures as low as in the case of earlier NANOBAIN steels has been achieved, even for the 0.6C family, where the lower C content, i.e. higher M_S and B_S, was compensated by higher Cr and Mn levels, as presented in Table 1**.**

4.4Enhanced transformation kinetics

One of the biggest problems that the benchmark alloys face in terms of practical industrial use is the time needed to complete the bainitic transformation at such low temperatures, which in some cases is up to 3 days [8]. The rate of reaction, controlled by the transformation driving force, was a key factor during the design process because transformation must be achieved in a realistic time. Thus, $\Delta G^{\gamma\rightarrow\alpha}$ was used to tailor the chemical compositions in such a way that the transformation times were reduced. In Fig. 5 and Fig.6 dotted lines represent the time needed to complete the transformation at different T for the fastest bench mark alloys (B.A.) [8]. The results indicate that, in general, the new alloys undergo faster transformation than the reference alloys. For the 1C &0.8C alloys, the transformation time at 200 ºC varies from 55-32 h, 1CMo and 1CSi, respectively, for the same alloys an increase of only 20 ºC in the transformation temperature implies a drastic decrease to 32 and 19 h respectively, keeping in mind that the benchmark alloys need at 200 ºC 72h to finish the transformation the achieved acceleration of the transformation is remarkable. At the intermediate T range of 240-300 ºC, the fastest of the new alloys take about 5 h and 7 h at 300 ºC and 240/260 ºC, 1CNb and 1CMo, respectively. This is a moderate acceleration when compared with the best of the benchmark alloys (8 and 10 h for the same T range). Lower C content in the 0.6C family, in principle, would imply faster transformation, an effect that is partially masked by the increase in Cr and Mn content in their chemical composition.

Another approach taken during the design stage to increase the transformation rate was to control the previous austenite grain size (PAGS). As bainite nucleates primarily in the austenite grain boundaries, a

decrease in PAGS will ensure an increase in the potent nucleation sites for bainitic ferrite [8]. With this aim in mind two alloys with Nb (1CNb and 0.6CNb) were designed. Nb through its carbides should exert control of the PAGS even at high temperatures, according to the theoretical calculations, by means of MTData [25]. At the austenizitation temperature of 950 ºC all the Nb should be precipitate as carbides; see Fig. 12.

For the sake of comparison, the average PAGS and its distribution have been measured in the 1C and the 1CNb alloys to evaluate if the approach of microalloying with sufficient quantities of carbide formers as Nb could indirectl, affect the kinetics of bainitic transformation. The PAGS results are presented in Fig

. 13, and it is evident that Nb exerts a pinning effect on the austenite grain size during austenitization. On the other hand, the kinetics results shown in Fig. 5 reveal that there is no clear trend. iIndeed there is an acceleration of the transformation at the highest transformation temperature, but at 200 ºC the 1C alloy is faster than the 1CNb even though PAGS is five times bigger. Assuming the same PAGS growth control by Nb carbides, similar uncertainty in the kinetics results is revealed when 0.6C and 0.6CNb data are compared, as presented in Fig. 6.

However, the full potential of such procedure, reducing PAGS, might be masked by the influence of other factors, such as the strength of austenite, i.e. chemical composition. It seems reasonable to assume that a stronger austenite will require more energy for ferrite plate growth, i.e. slowing down the transformation. We speculate that the effect of the PAGS on the transformation kinetics might be more evident when comparing the same steel with large and small PAGS, as in ref. [8].

4.5Hardenabillity

As mentioned, the designed alloys are intended for components with very different sizes, and it was calculated and considered during the design process that even at the slowest cooling point of the aimed

components, 1.5 ºC/s, the cooling rate should be sufficient to avoid formation of ferrite/pearlite or other transformation products during cooling to the transformation temperature. From the obtained CCT, as seen in Fig. 2, it was possible to estimate that for the 1C & 0.8C family, hardenability (the critical CR in Table 2) is largely below that of the 0.6C alloys, between 3-5 ºC/s, and in both cases it is higher than the level originally targeted during the design process, 1.5 ºC/s. The discrepancies between experimental and theoretical hardenability values might be due to the strong influence that PAGS has on the latter, and influence that the theoretical approach used for hardenability purposes cannot take into account [33]. Nevertheless, the alloys were found within the tolerance limits for the components aimed at originally: 1C & 0.8C family for small components and 0.6C for bigger components.

4.6Additional refinement of the microstructure

Bainite plate thickness is mainly controlled by the strength of the austenite from where it grows [13,34]. The novel approach in this work is aimed at directly acting on the strength of the parent austenite by including strong solid solution strengtheners as Si (1CSi) and Mo (1CMo,0.6CMo). Results in Table 3 indicate that additions of Mo and Si are an effective way to decrease the bainitic ferrite plate thickness, when compared, for example, with 1C or 0.8C alloys. The reduction is significantly higher when comparing 0.6C and 0.6Mo, with decreasing plate thickness from 60 to 43 nm, respectively. The increase in Cr and decrease in Mn, the 0.6CCr as compared with 0.6C, offers an opportunity to assess the Cr capability in hardening austenite i.e. decreasing the plate thickness, 60 nm for the latter as compared with 43 nm for the former. As C is the element with the strongest hardening capacity in austenite after N [16,35], it is natural that its reduction in the 0.6C family leads to a thickening of the bainitic ferrite plates when compared with the 1C-0.8C family; see Table 3.

Although the temperature range is limited and corresponds to the lower transformation temperature regime, the results in Table 3 lead to two more conclusions: (i) the new results appear to be insensitive to

transformation temperature (a decrease in plate thickness is expected when transformation T decreases) and (ii) the plate thickness is similar to that reported among the 1C & 0.8C family. The same conclusions might be derived when results from the benchmark alloys (B.A.) in ref. 8 are analyzed. We speculate that a limit in the minimum attainable plate thickness might exist, and further research on this topic is in progress. Finally, comparison of the results of the benchmark alloys [6,8] with those in Table 3 show that additional refinement of the plate thickness has been attained.

5.CONCLUSIONS

It has been experimentally demonstrated that it is possible to obtain nanocristalline bainite in simpler alloy systems and in shorter times than those reported to date for NANOBAIN alloys. Moreover, these advances will help industrial demands for practical application of NANOBAIN. In particular, specific hardenability requirements for application were considered by tailoring the alloy composition.

The experimental results validate the design approach followed in this study, based on phase transformation theory and basic metallurgical concepts, and illustrate that the NANOBAIN concept is closer to industrialization.

ACKNOWLEDGEMENTS

The authors gratefully acknowledge the support of the European Research Fund for Coal and Steel and the Spanish Ministerio de Economia y Competitividad Plan Nacional de I+D+I (2008-2011) for funding this research under contracts RFSR-CT-2008-00022, and MAT2010 – 15330, respectively. J. Cornide also acknowledges the Spanish Ministry of Science and Innovation for financial support in the form of a PhD research grant (FPI).

REFERENCES

1. C. Garcia-Mateo and H. K. D. H. Bhadeshia, *Mater. Sci. Eng. A* **378**, 289 (2004).
2. G. B. Olson and M. Cohen, *Metall. Trans. A* **7**, 1897 (1976).
3. H. K. D. H. Bhadeshia, *Bainite in Steels. Transformations, Microstructure and Properties*, Institute of Materials, Minerals and Mining, London (2001).
4. H. K. D. H. Bhadeshia, *Acta Metall.* **29**, 1117 (1981).
5. H. K. D. H. Bhadeshia and A. R. Waugh, *Acta Metall.* **30**, 775 (1982).
6. C. Garcia-Mateo, F. G. Caballero and H. K. D. H. Bhadeshia, *ISIJ Int.* **43**, 1238 (2003).
7. F. G. Caballero, H. K. D. H. Bhadeshia, K. J. A. Mawella, D. G. Jones and P. Brown, *Mater. Sci. Technol.* **18**, 279 (2002).
8. C. Garcia-Mateo, F. G. Caballero and H. K. D. H. Bhadeshia, *ISIJ Int.* **43**, 1821 (2003).
9. H. I. Aaronson, H. A. Domian and G. M. Pound, *Trans. Metall. AIME* **236**, 781 (1966).
10. F. G. Caballero, H. K. D. H. Bhadeshia, K. J. A. Mawella, D. G. Jones and P. Brown, *Mater. Sci. Technol.* **17**, 517 (2001).
11. C. Garcia-Mateo and F. G. Caballero, *ISIJ Int.* **45**, 1736 (2005).
12. E. Kozeschnik and H. K. D. H. Bhadeshia, *Mater. Sci. Technol.* **24**, 343 (2008).
13. S. B. Singh and H. K. D. H. Bhadeshia, *Mater. Sci. Eng. A* **245**, 72 (1998).
14. H. K. D. H. Bhadeshia and D. V. Edmonds, *Met. Sci.* **17**, 411 (1983).
15. V. Heuer, K. Löser and J. Ruppel, *HTM Haerterei Tech. Mitt.* **64**, 28 (2009).
16. C. H. Young and H. K. D. H. Bhadeshia, *Mater. Sci. Technol.* **10**, 209 (1994).
17. F. G. Caballero, H. K. D. H. Bhadeshia, K. J. A. Mawella, D. G. Jones and P. Brown, *Mater. Sci. Technol.* **17**, 512 (2001).
18. F. G. Caballero, M. J. Santofimia, C. Capdevila, C. García-Mateo and C. De García Andrés, *ISIJ Int.* **46**, 1479 (2006).
19. C. Garcia-Mateo and F. G. Caballero, *Int. J. Mater. Res.* **98**, 137 (2007).
20. F. G. Caballero, M. K. Miller, C. Garcia-Mateo, C. Capdevila and C. Garcia de Andrés, *JOM* **60**, 16 (2008).
21. L. C. Chang and H. K. D. H. Bhadeshia, *Mater. Sci. Technol.* **11**, 874 (1995).

22. C. G. de Andres, F. G. Caballero, C. Capdevila and D. San Martin, *Mater. Charact.* **49**, 121-127 (2002).
23. C. G. de Andres, M. J. Bartolome, C. Capdevila, D. S. Martin, F. G. Caballero and V. Lopez, *Mater. Charact.* **46**, 389-398 (2001).
24. C. Garcia-Mateo, F. G. Caballero, M. K. Miller and J. A. Jimenez, *J. Mater. Sci.* **47**, 1004-1010 (2012).
25. MTDATA, NPL Software Tool for the Calculation of Phase Equilibria and Thermodynamic Properties, National Physical Laboratory, Teddington, United Kingdom, 2006.
26. J. W. Cahn and W. C. Hagel, *Decomposition of austenite by diffusional processes*, John Wiley, New York (1962).
27. A. S. Pandit, *Theory of the Pearlite Transformation in Steels*, University of Cambridge(2011).
28. H. K. D. H. Bhadeshia and D. V. Edmonds, *Metall. Trans. A* **10**, 895-907 (1979).
29. L. C. Chang and H. K. D. H. Bhadeshia, *Mater. Sci. Technol.* **11**, 105-108 (1995).
30. I. B. Timokhina, H. Beladi, X. Y. Xiong, Y. Adachi and P. D. Hodgson, *Acta Mater.* **59**, 5511-5522 (2011).
31. E. Pereloma, H. Beladi, L. Zhang and I. Timokhina, *Metall. Mater. Trans. A* **43**, 3958-3971 (2012).
32. F. G. Caballero, H. W. Yen, M. K. Miller, J. R. Yang, J. Cornide and C. Garcia-Mateo, *Acta Mater.* **59**, 6117-6123 (2011).
33. H. K. D. H. Bhadeshia, *Met. Sci.* **16**, 159-165 (1982).
34. J. Cornide, C. Garcia-Mateo, C. Capdevila and F. G. Caballero, *J. Alloys Compd.* (2012) DOI:10.1016/j.jallcom.2011.11.066.
35. K. J. Irvine, T. Gladman and P. F. B., *J. Iron Steel Inst.* **207**, 1017-1028 (1969).

1 TABLE CAPTIONS AND TABLES

Table 1. Actual chemical composition of selected alloys (wt.%).

Table 2. Characteristic transformation temperatures for all laboratory alloys investigated. Ac3 must be understood as Acm for high C grades. Critical CR refers to the highest cooling rate at which ferrite/pearlite appears in the microstructure.

Table3. Microstructural parameters for all investigated specimens. T is the temperature of the isothermal heat treatment, t_b is the bainitic ferrite plate thickness, and V_γ is the austenite volume fraction.

Table 1.Actual chemical composition of selected alloys (wt.%).

Steel	C	Si	Mn	Cr	Mo	Nb
1C	0.99	1.58	0.76	0.45		
1CNb	1.00	1.53	0.75	0.51		0.02
1CMo	1.01	1.51	0.82	0.46	0.096	
1CSi	0.98	2.90	0.77	0.45		
0.8C	0.88	1.54	0.69	0.50		
0.6C	0.67	1.6	1.25	1.50		
0.6CCr	0.61	1.45	0.76	2.42		
0.6CNb	0.64	1.60	1.27	1.5		0.03
0.6CMo	0.58	1.63	1.29	1.43	0.1	

Table 2. Characteristic transformation temperatures for all laboratory alloys investigated. Ac3 must be understood as Acm for high C grades. Critical CR refers to the highest cooling rate at which ferrite/pearlite appears in the microstructure.

	Ac1/ºC	Ac3/ºC	M_S/ºC	Critical CR/ ºC/s
1C	742	880	130	20
1CMo	742	880	130	15
1CNb	741	881	123	20
1CSi	769	893	165	20
08C	758	808	165	13
06C	770	838	217	5
06CMo	795	853	220	3
06CNb	766	840	207	5
06CCr	808	872	240	5

Table 3. Microstructural parameters for all investigated specimens. T is the temperature of the isothermal heat treatment, tb is the bainitic ferrite plate thickness, and V_γ is the austenite. volume fraction.

	T/ºC	t_b/nm	V_γ □±3□/%
1C	250	38	20
1CMo	250	32	22
1CMo	220	32	25
1CMo	200	21	20
1CNb	240	28	21
1CNb	220	30	23
1CSi	250	28	33
1CSi	220	28	36
08C	270	36	24
08C	250	37	18
08C	220	35	16
06C	250	60	12
06CMo	250	43	20
06CNb	250	65	18
06CNb	220	60	27
06CCr	250	43	19

2 FIGURE CAPTIONS AND FIGURES

Figure 1. Theoretical isopleth for XC-2.5Si-0.75Mn-0.5Cr, all in wt.%.

Figure 2. Experimental CCT diagrams for (a) 0.6CCr, (b) 0.6Mo and (c) 1CSi, alloys. P stands for pearlite, M for martensite and the numerical values at the end of cooling curves are the measured HV. Also presented are the experimental Ac1, Ac3, and MS temperatures obtained from the dilatometric curves.

Figure 3. Isothermal transformation kinetics for (a) 1C and (b) 0.6CCr alloys.

Figure 4. Schematic representation showing the procedure used to estimate the end of bainitic transformation.

Figure 5. Time to fully transform the 1C & 0.8C grades, as a function of transformation temperature. Also presented for the same conditions, hardness as a function of transformation temperature. Dotted lines represent the values obtained for the best of the benchmark alloys (B.A.) selected during the design process [8].

Figure 6. Time to fully transform the 0.6C grades as a function of transformation temperature. Also presented for the same conditions, hardness as a function of transformation temperature. Dotted lines represent the values obtained for the best of the benchmark alloys (B.A.) selected during the design process [8].

Figure 7. Optical microscopy micrographs showing examples of the 1C alloy bainitic microstructure obtained by isothermal transformation (a) 220 ºC and (b) 300 ºC.

Figure 8. FEG-SEM micrographs showing examples of various bainitic microstructures obtained by isothermal transformation at 220 ºC of (a) 0.8 C alloy and (b) 1CSi alloy.

Figure 9. TEM micrographs of the microstructure obtained in the 1CSi alloy after transformation at 200 ºC.

Figure 10. Retained austenite morphologies distribution and average width.

Figure 11. Experimental results on the MS temperature and the highest tested temperature where bainite was obtained. NANO# corresponds to the NANOBAIN steel family described in ref. 6 (#2) and ref. 8 (#3 &4).

Figure 12. Theoretical calculation of the amount of Nb carbide (C0.877Nb) as a function of temperature for the 1CNb alloy.

Figure 13. PAGS distribution and average value for the 1C and 1CNb alloys.

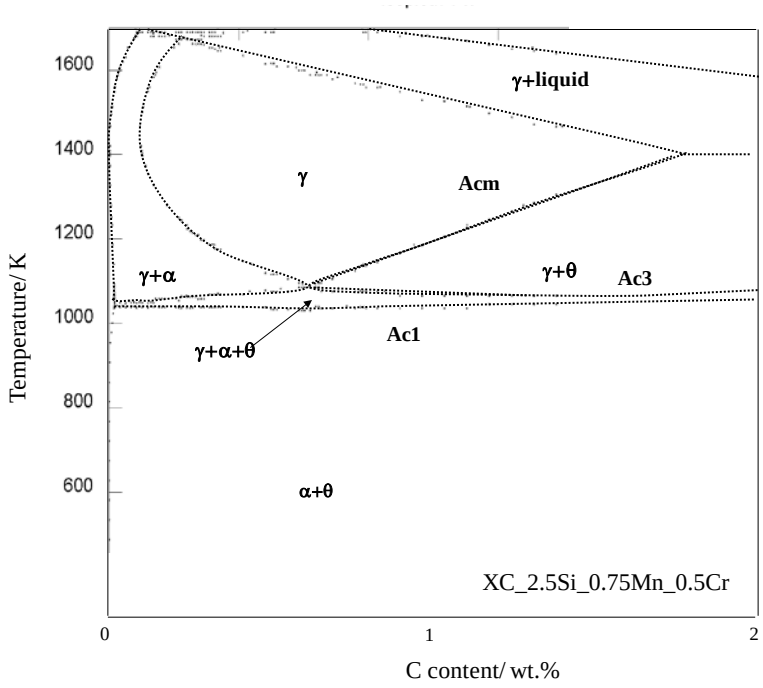

Figure 1. Theoretical isopleth for XC-2.5Si-0.75Mn-0.5Cr all in wt.%.

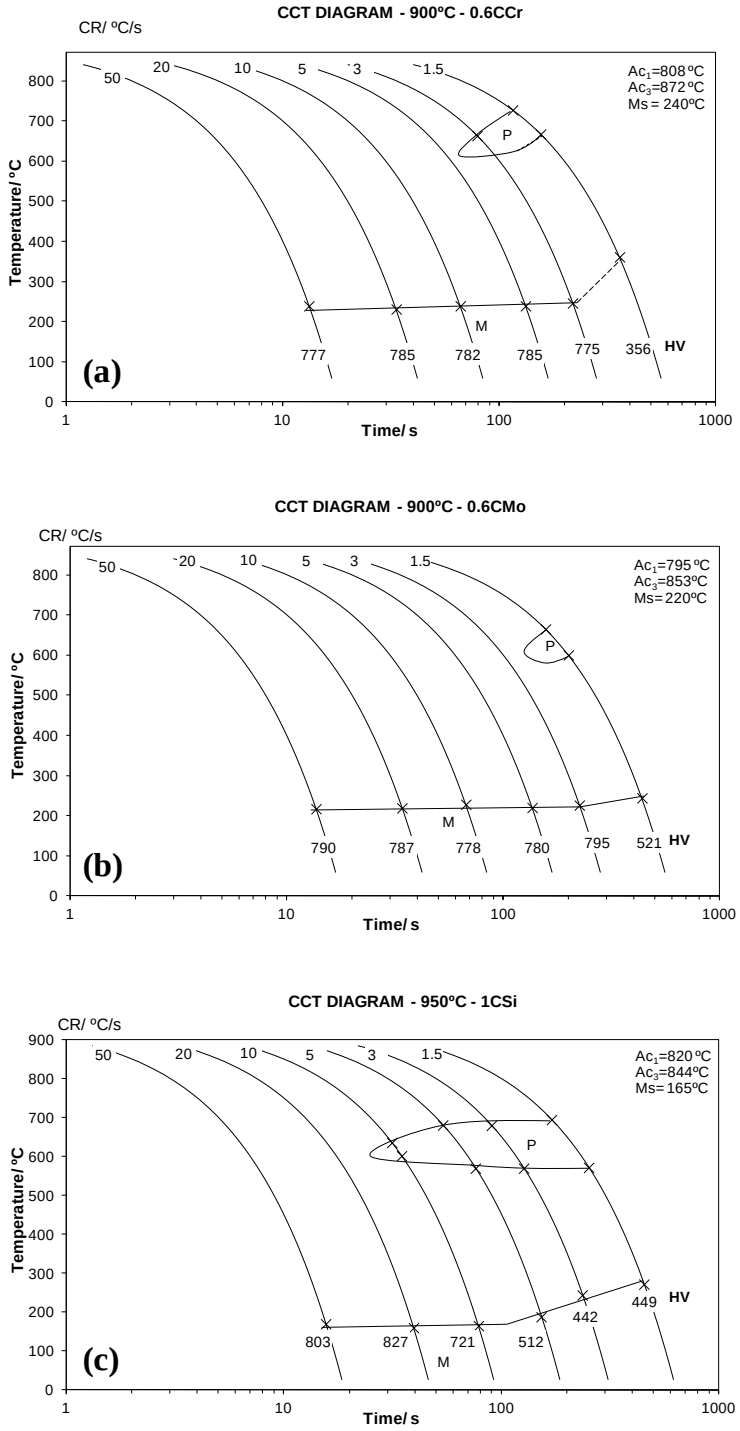

Figure 2. Experimental CCT diagrams for (a) 0.6CCr, (b) 0.6Mo and (c) 1CSi, alloys. P stands for pearlite, M for martensite and the numerical values at the end of cooling curves are the measured HV. Also presented the experimental A_{c1}, A_{c3} and M_S temperatures obtained from the dilatometric curves.

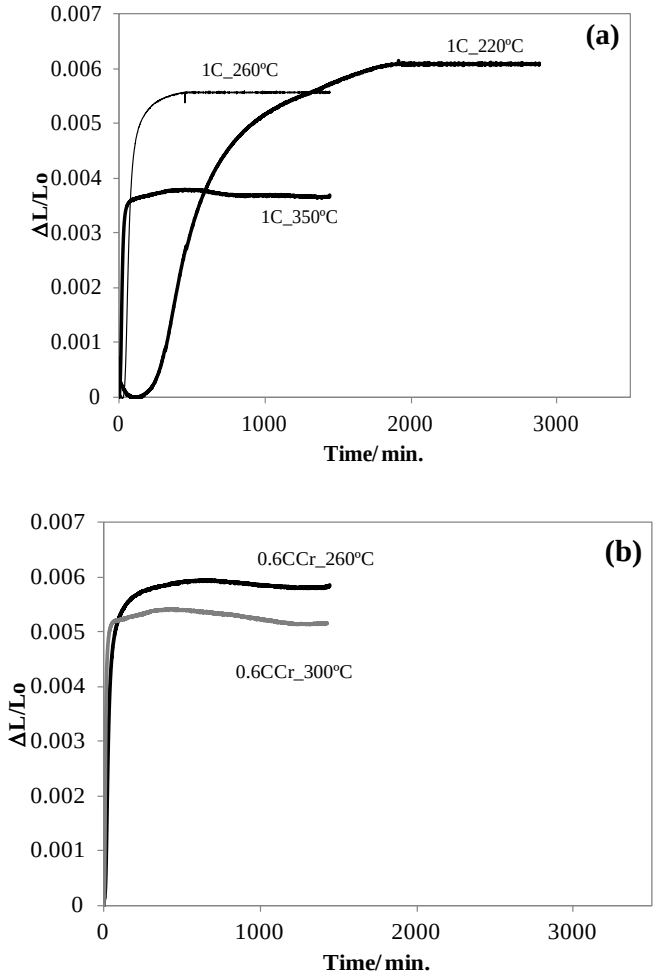

Figure 3. Isothermal transformation kinetics for (a) 1C and (b) 0.6CCr alloys.

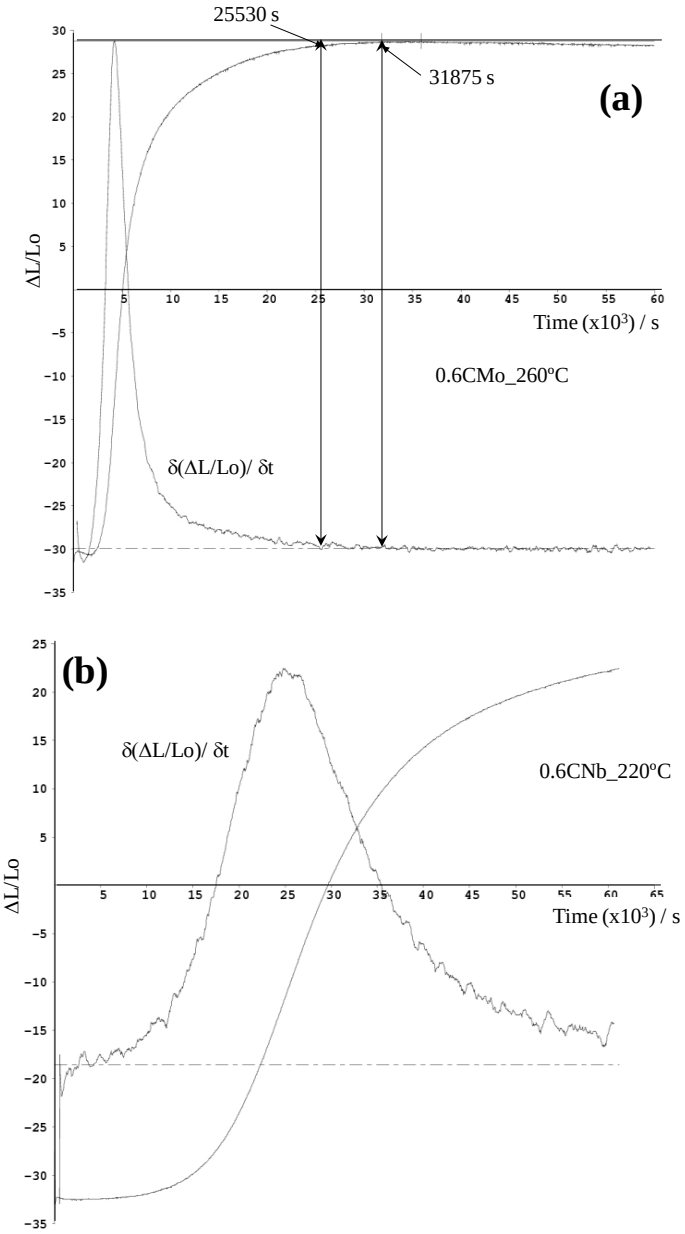

Figure 4. Schematic representation showing the procedure used to estimate the end of bainitic transformation.

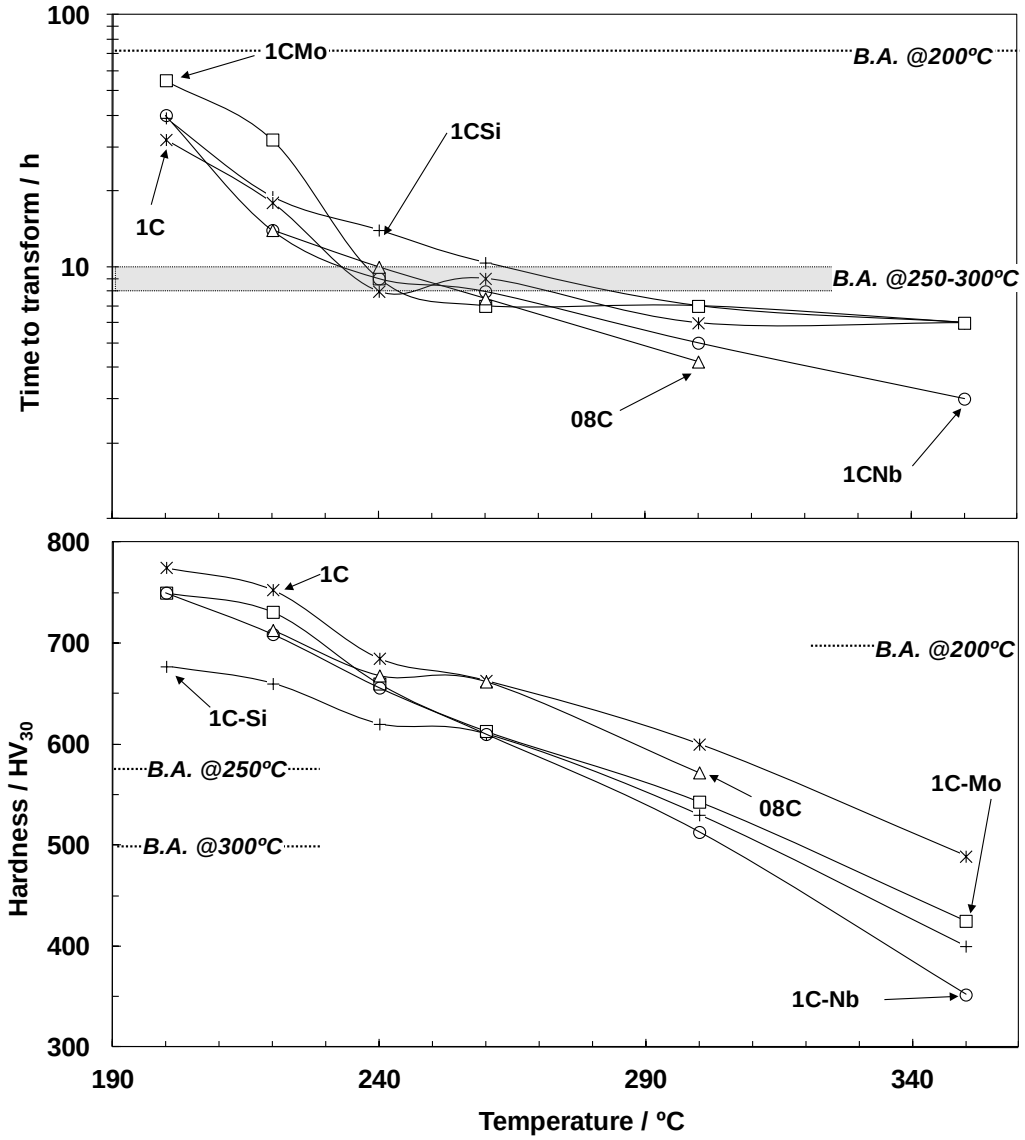

Figure 5. Time to fully transform the 1C & 0.8C grades, as a function of transformation temperature. Also presented for the same conditions, hardness as a function of transformation temperature. Doted lines represent the values obtained for the best of the benchmark alloys (B.A.) selected during the design process [3].

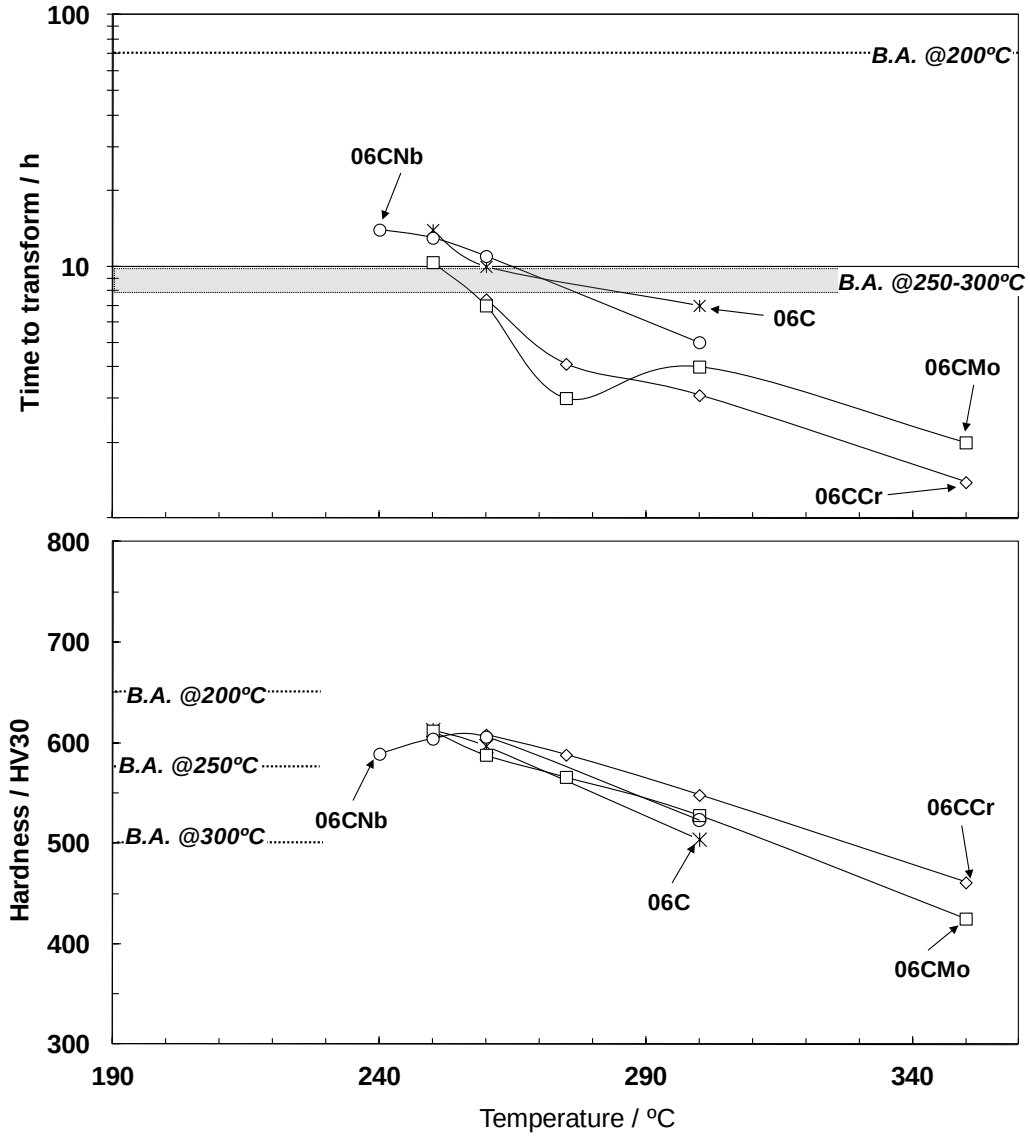

Figure 6. Time to fully transform the 0.6C grades as a function of transformation temperature. Also presented for the same conditions, hardness as a function of transformation temperature. Doted lines represent the values obtained for the best of the benchmark alloys (B.A.) selected during the design process [3].

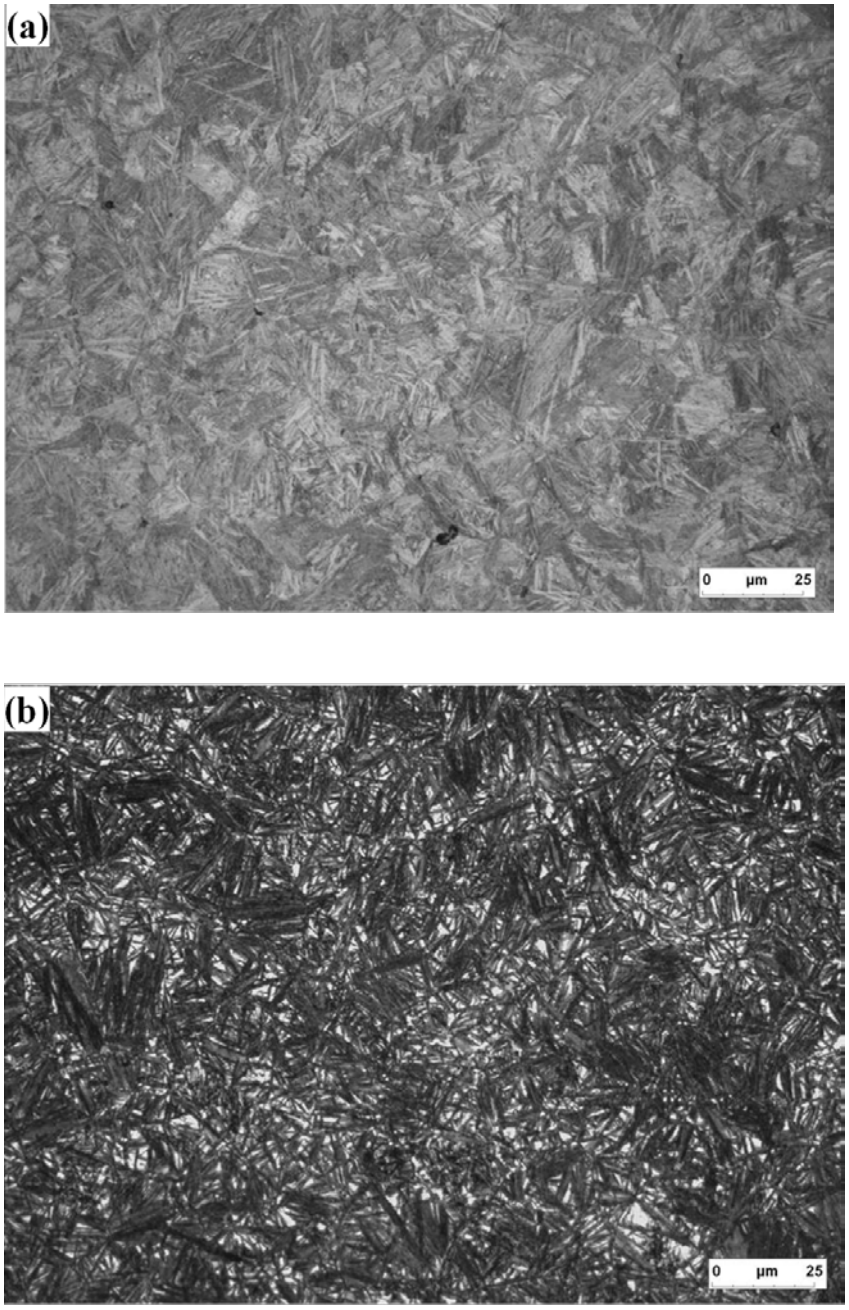

Figure 7. Optical microscopy micrographs showing examples of the 1C alloy bainitic microstructure obtained by isothermal transformation (a) 220ºC and (b) 300ºC.

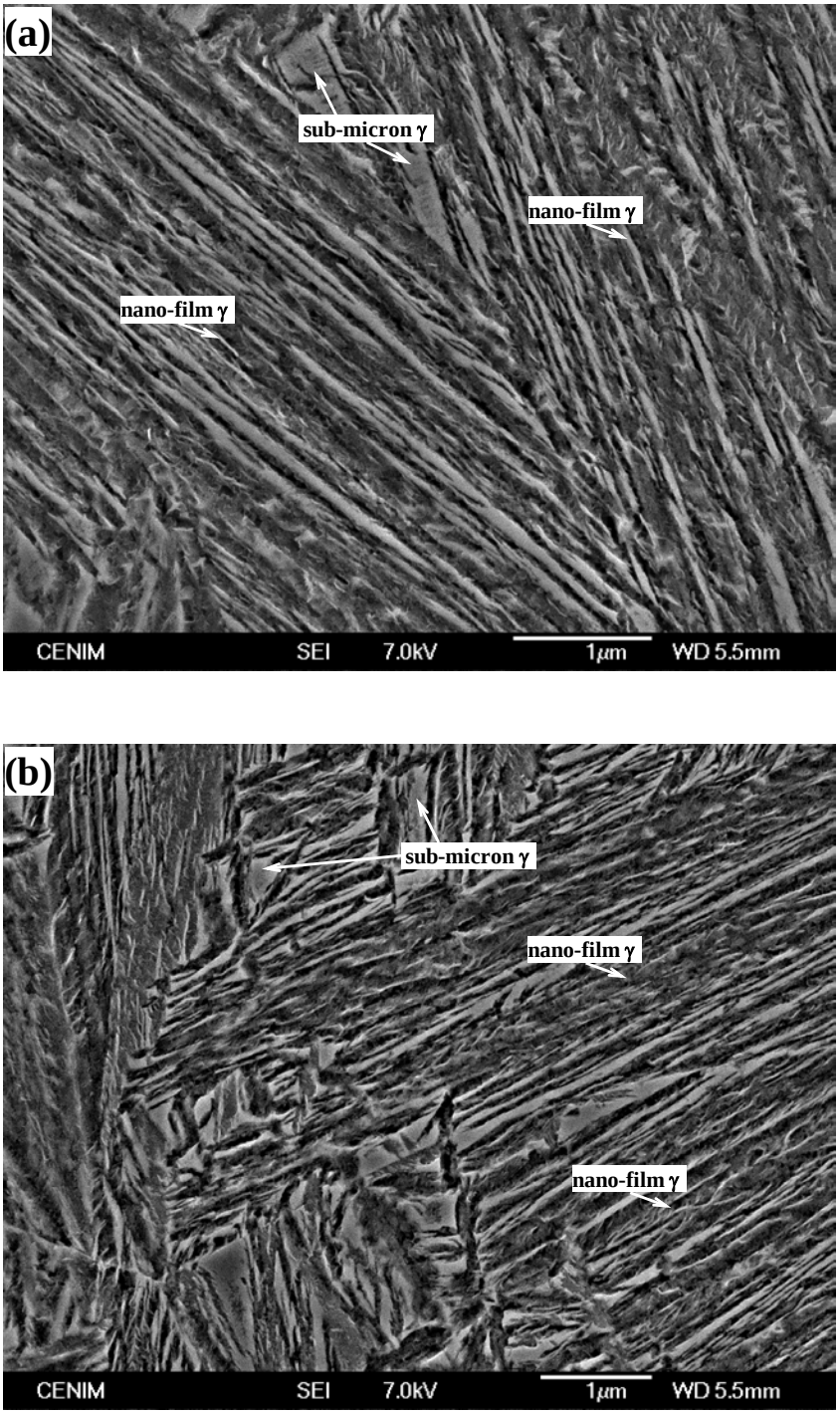

Figure 8. FEG-SEM micrographs showing examples of various bainitic microstructures obtained by isothermal transformation at 220ºC of (a) 0.8 C alloy and (b) 1CSi alloy.

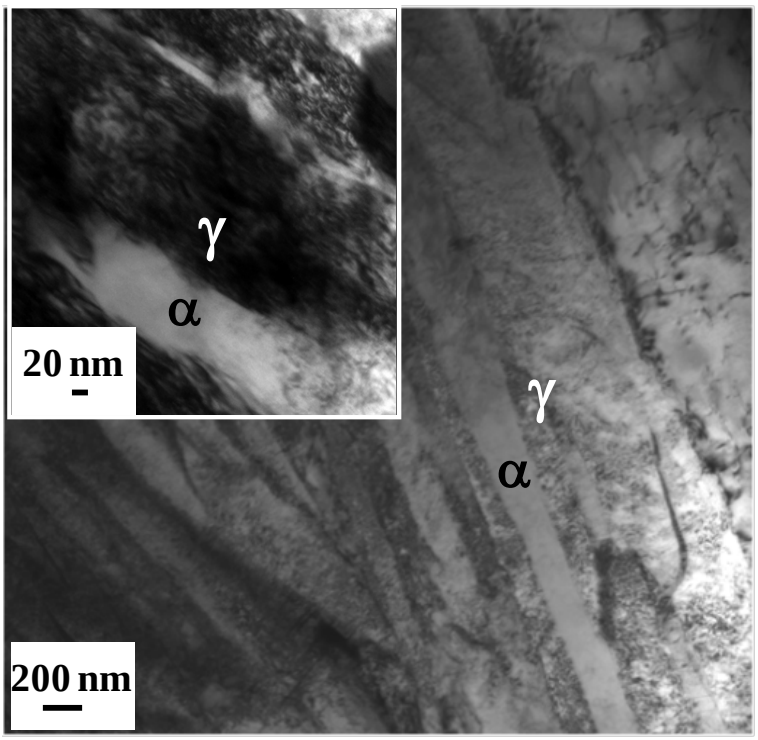

Figure 9. TEM micrographs of the microstructure obtained in the 1CSi alloy after transformation at 200ºC.

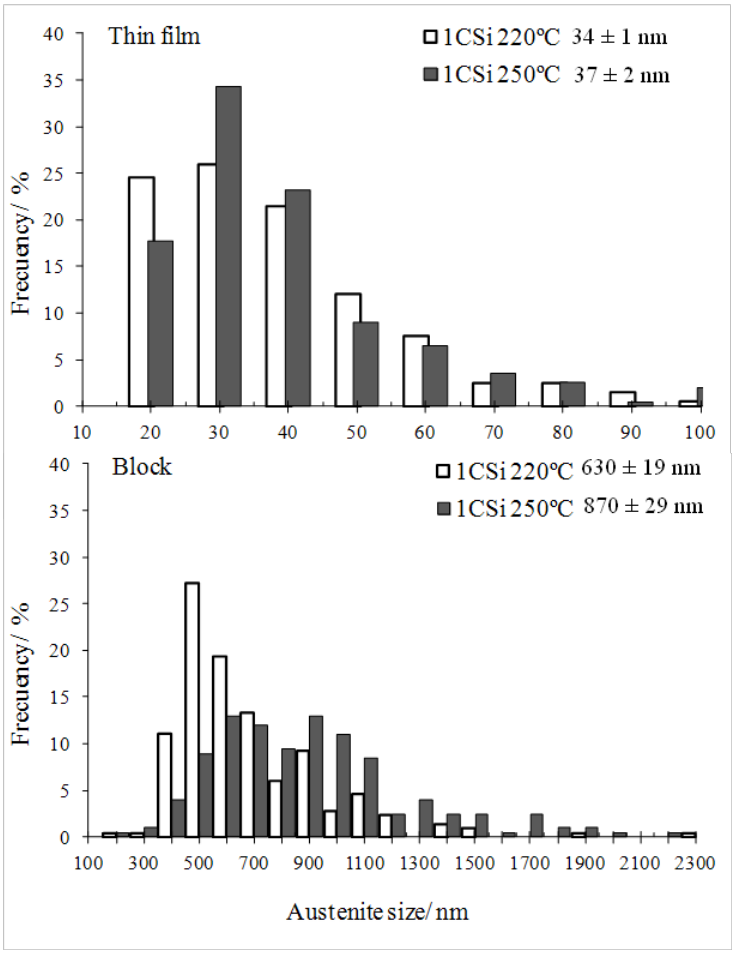

Figure 10. Retained austenite morphologies distribution and average size.

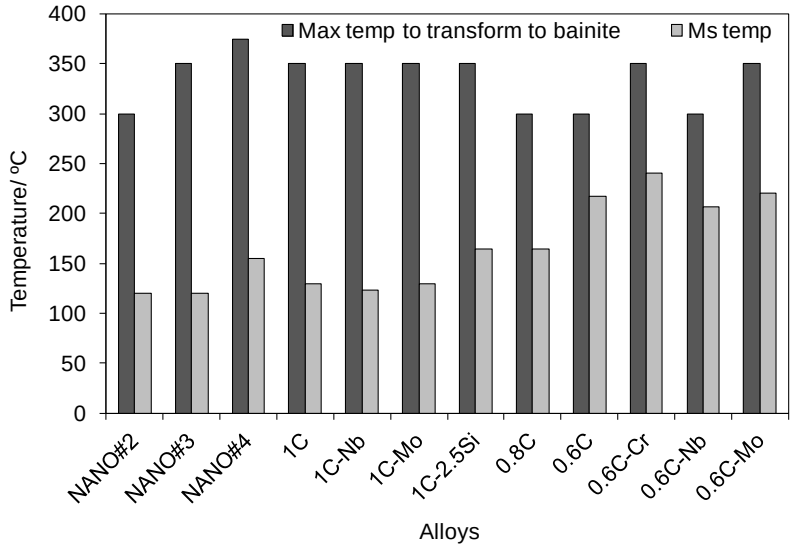

Figure 11. Experimental results on the M_S temperature and the highest tested temperature where bainite was obtained. NANO# corresponds to the NANOBAIN steel family described in ref. 1 (#2), and ref. 3 (#3 &4).

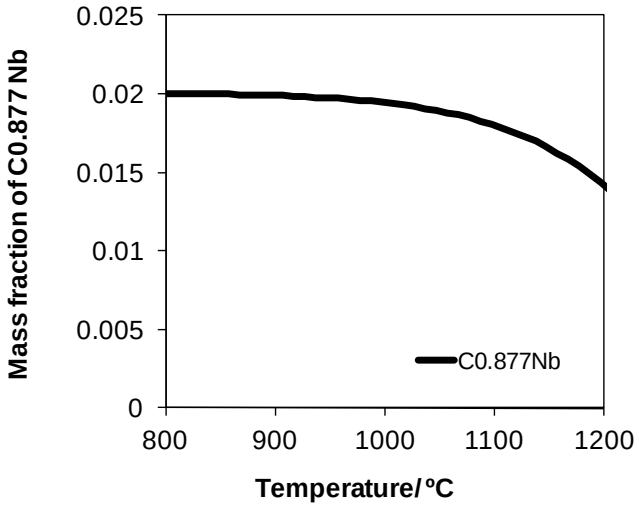

Figure 12. Theoretical calculation of the amount of Nb carbide (C0.877Nb) as a function of temperature for the 1CNb alloy.

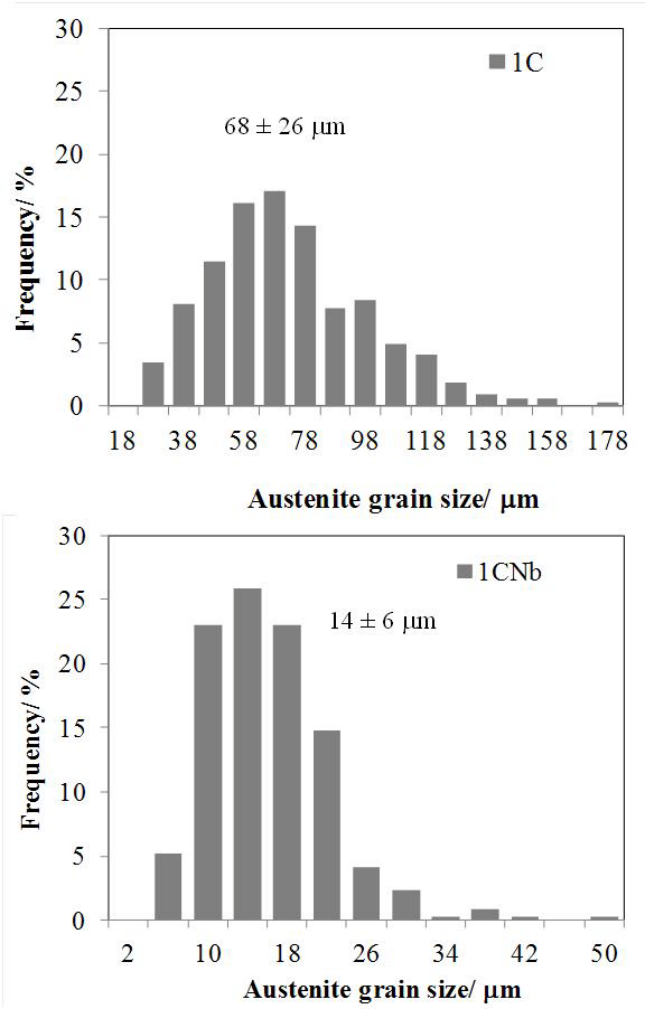

Figure 13. PAGS distribution and average value for the 1C and 1CNb alloys.